Optical and Quantum Electronics (2019) 51:396
https://doi.org/10.1007/s11082-019-2117-0

Modeling of dielectric function in plasmonic quantum dot nanolaser

Jamal N. Jabir[1,2,3] · **S. M. M. Ameen**[1] · **Amin Habbeb Al-Khursan**[2]

Received: 3 September 2019 / Accepted: 13 November 2019

Abstract
In this work we present a model of the dielectric function in plasmonic quantum dot (QD) nanolaser. A metal/semiconductor/metal structure was considered to attain plasmonic nanocavity with active region containing: QD, wetting layer and barrier. The dielectric function was calculated for both metal (Ag) and QD structure. The propagation constant of surface plasmon polariton (SPP) at the interface of Ag/InAs-QD structure was calculated and the dispersion relation of the plasmonic QD structure was evaluated. For frequencies far from plasma one, the gap between real and imaginary parts was large and a deviation from linear relation was obvious. The SPP field was strongly localized at the interface due to the effect of zero-dimensional QD structure which has application in the super-resolution and best sensitivity in optical imaging. Results of propagation length of SPP (L_{spp}) also support this. According to the L_{spp} results, the damping in the SPP energy was low in the Ag/InAs-QD compared to that in the Ag/air interface. The obtained results are in the range of experimental ones.

Keywords Surface plasmon polariton · Ag/QD · Plasmonic QD structure

1 Introduction

Enormous device applications like true nanolasers, detectors, and solar cells with unexpected performance depend on reducing the cavity dimensions. For example, nanolasers are of low power consumption and have important applications such as biosensing and optical logic circuits with fast-switching (Ni et al. 2011). Reducing the cavity (or waveguide) dimensions to a nanoscale is not possible with conventional dielectric waveguides due to losses resulting from the low optical confinement of the mode. This challenge is possible by integrating semiconductor nanostructures with a metallic cavity. This results

✉ Amin Habbeb Al-Khursan
ameen_2all@yahoo.com

1 College of Science, University of Basrah, Basrah, Iraq

2 Nassiriya Nanotechnology Research Laboratory (NNRL), Science College, Thi-Qar University, Nassiriya, Iraq

3 Department of Physics, College of Education, University of Al-Qadisiyah, Diwaniyah, Iraq

Published online: 19 November 2019

in what is called plasmonic nanolaser. But, the metal losses are reducing the propagation length. Thus, high gain active region is required (Li and Ning 2009).

Surface plasmon-polaritons (SPPs) refers to the wave that includes both charge motion in metal (surface plasmons) and the electromagnetic waves in the dielectric (polaritons) (Zeng et al. 2014). SPPs are surface electromagnetic waves that are coupled with free electron density oscillations bounded and propagated along with the interface between metal and dielectric (or semiconductor) (Han et al. 2018; Berini and Leon 2012; Dionne et al. 2005).

Quantum dots (QDs) can be taken as the high gain in a plasmonic nanolaser, which balances between the loss of metal and gain in a metal–semiconductor–metal (MSM) structure (Holmström et al. 2010; Li and Ning 2009). This is because QD possesses discrete energy states resembling those in natural atoms or molecules, QDs are regarded as a zero-dimensional structure where the electronic motion is confined in all three spatial dimensions. They exhibit unexpected characteristics due to their incredibly small size with quantum mechanical behavior (Dwara and Al-Khursan 2015).

The strucuture we studied contains a InAs QD grown on a wetting layer (WL) sourended by a GaAs barrier (B). The WL is in the form of a quantum well (Bimberg et al. 1997; Kim and Chuang 2006; Kim et al. 2008).

The dielectric constant $\varepsilon(\omega)$ gives almost the entire information of material, such as transitions and attenuation coefficient in metals through infrared, visible, and ultraviolet photon energies (Vargas 2017), reflectivity (Rakic et al. 1998), and optical gain of the semiconductors (Wijesinghe and Premaratne 2012). Accordingly, this work is modeling the dielectric function in a polasmonic QD nanolaser. Here, it is shown that the SPP field is strongly localized at the interface of metal-Ag/InAs-QD due to the effect of zero-dimensional QD structure. The obtained results of propagation length of SPP, L_{spp}, also support this. This has applications in the super-resolution and high sensitivity optical imaging. L_{spp} results also asserts that the damping in the SPP energy was low in the Ag/InAs-QD compared to that in the Ag/air interface. The obtained results are in the range of experimental ones. This work was organized as follows: Sect. 2 discusses the surface plasmon-polariton behavior, Sect. 3 develops the dielectric function for plasmonic QD structure. Section 4 states the propagation length and skin depth relations. Section 5 describes the plasmonic QD structure studied in this work. The results are discussed in Sect. 6, while the conclusions were drowned in Sect. 7.

2 Surface plasmon-polaritons behavior

All the SPP features can be derived from Maxwell's equations, where SPPs are TM-modes, in other words (E_x, E_z, $H_y \neq 0$ and E_y, H_x, $H_z = 0$). The dielectric function of plasmonic QD structure must consist both metal and QD contributions. So, it can be written as,

$$\varepsilon(\omega) = \varepsilon_m + \varepsilon_{QD} \tag{1}$$

Note that $\varepsilon(\omega)$ is the dielectric function of the overall structure (plasmonic QD structure), ε_m is the dielectric function of the metal, while ε_{QD} is the dielectric function of QDs.

To create SPPs, the real part of the metal dielectric function should be negative (Raether 1988). The electromagnetic waves, that pass through metal, are suffering from the decay due to ohmic losses. In order to describe SPP characteristics, different models are used such as the Drude model (Chen et al. 2004). Suppose that the first medium is metal with ε_m

and the another is a QD with ε_{QD} (the real part of the dielectric constant of semiconductor QD is ε'_{QD}) then, the dispersion relation for a wave propagating along the interface between metal/dielectric was given by (Raether 1988; Lüth 2015; Homola 2003),

$$k_{SPP} = \frac{\omega}{c}\left[\left(\frac{\varepsilon'_m \varepsilon'_{QD}}{\varepsilon'_m + \varepsilon'_{QD}}\right)^{1/2} + j\left(\frac{\varepsilon'_m \varepsilon'_{QD}}{\varepsilon'_m + \varepsilon'_{QD}}\right)^{3/2} \frac{\varepsilon'_m}{2(\varepsilon'_m)^2}\right] \tag{2}$$

where k_x is a complex wavevector, ω is the SPP frequency, c is the light speed in vacuum, and j is the imaginary number. In general case, electromagnetic field stimulates electron oscillations and collisions was result in damping which causes losses in metal that cannot be avoided. They are represented by a collisional rate $\gamma_p = 1/\tau$ with τ is the relaxation time of free electrons. So, the frequency-dependent dielectric function in metal is given by (Mishchenko et al. 2002; Maier 2007),

$$\varepsilon_m(\omega) = 1 - \frac{\omega_p^2}{\omega(\omega + j\gamma_p)} \tag{3}$$

which is the Drude model. Note that, ω_p is the bulk plasma frequency. It is given by (Kittel 2005),

$$\omega_p = \sqrt{\frac{n\, e^2}{\varepsilon_\circ\, m_e^*}} \tag{4}$$

where n is the number of electrons, e is the elementary charge, $\varepsilon_\circ$ is the free space permittivity, and m_e^* is effective electron mass. The metal dielectric function is written as,

$$\varepsilon_m = \varepsilon'_m + j\varepsilon'_m \tag{5}$$

with $\left|\varepsilon'_m\right| \gg \varepsilon''_m$, where ε'_m and ε''_m are real and imaginary parts of the dielectric function, respectively. Since QDs as a very small growing nanostructures are taken as lossless ($\varepsilon''_{QD} = 0$) (Homola 2003; Al-Khursan 2006). This assumption is checked in the following results as referred to thereafter.

3 Dielectric function of plasmonic QD structure

Since the susceptibility $\chi(\omega)$ is related to the dielectric function $\varepsilon(\omega)$ through the expression (Sernelius 2001),

$$\chi(\omega) = \frac{\varepsilon(\omega)}{\varepsilon_0} - 1 \tag{6}$$

Then the dielectric function of the plasmonic QD structure is,

$$\varepsilon(\omega) = \varepsilon_0 + \frac{\varepsilon_0 \omega_p^2}{\omega_0 - \omega^2 + j\omega\gamma_p} + \varepsilon_0(1 + \chi_{QD}(\omega)) \tag{7}$$

where the QD susceptibility is defined by (Bimberg et al. 1997),

$$\chi_{QD}(\omega) = \int_{-\infty}^{+\infty} \frac{2}{V} \frac{|M_{cv}|^2}{\hbar} \frac{(\rho_c - \rho_v)}{(\omega - \omega'_{cv} - j\gamma_{cv})} D(E')\mathrm{d}E' \tag{8}$$

with the inhomogeneous Gaussian density of states,

$$D(E') = \frac{2}{V_{dot}} \frac{1}{\sqrt{2\pi\sigma^2}} \exp\left(\frac{-(E' - E_{\max})^2}{2\sigma^2}\right) \tag{9}$$

M_{cv}, ρ_c, ρ_v, ω, ω_{cv}, $\gamma_{cv}(= 1/\tau_{cv})$ and ω_0 are the QD momentum matrix element, Fermi distribution functions of CB and VB, the frequency of the mode, interband transition energy in the QD, intraband relaxation rate in QD, resonance frequency, respectively. The remaining factor γ_p represents the collisional rate between metal electrons. Note that the resonance frequency in metal was zero ($\omega_0 = 0$). Note that $\gamma_p(1/p\,s)$= 41, and $\tau_{cv}(1/p\,s) = 4.1$ (Abdullah et al. 2015).

4 Skin depth and propagation length

When SPPs are propagated along with the metal/dielectric interface, they are losing energy into the metal due to the absorption (attenuation). SPP intensity is proportional to the square of the electric field. So, for a distance x, the intensity falls to $e^{-2k_{SPP}x}$ and the propagating length is defined as the maximum distance of SPPs to decay by $1/e$ of the original value. It is given by $L_{spp} = 1/2k''_{SPP}$ (Homola 2003, 2006). However, the distance that SPPs penetrates into the metal or dielectric medium is called skin depth δ_i. The index (i) refers to metal or dielectric ($i = m, d$). SPPs also attenuates evanescently perpendicular to the metal interface and can be quantified using the skin depth (Wu et al. 2017),

$$\delta_{m,QD} = \frac{\lambda}{2\pi} \left\{ \frac{|\varepsilon'_m| + \varepsilon'_{QD}}{(\varepsilon'_{m,QD})^2} \right\} \tag{10}$$

5 Plasmonic QD structure

The plasmonic QD structure studied in this work was composed of metal (silver Ag), barrier (GaAs), and QD (InAs) which is grown on the wetting layer (InGaAs). The QDs are taken in the form of quantum disks with radius of 14 nm and height 2 nm. The structure is shown in Fig. 1.

The energy subbands of the InAs QDs are calculated by solving the schrodinger equation under the assumption of parabolic bands. The QDs are assumed to be in the form of quantum disks. Such assumption is also used by others, for example see (Kim and Chuang 2006; Kim et al. 2008). It is also checked with experimental results (Al-Husseini et al. 2009). The QD susceptibility χ_{QD} is calculated from Eq. (8). The real and imaginary part of the dielectric functions of the metal and QDs are calculated, the skin depth, and L_{spp} are specified and k_{SPP} dispersion relation is plotted. All calculations are done under Matlab.

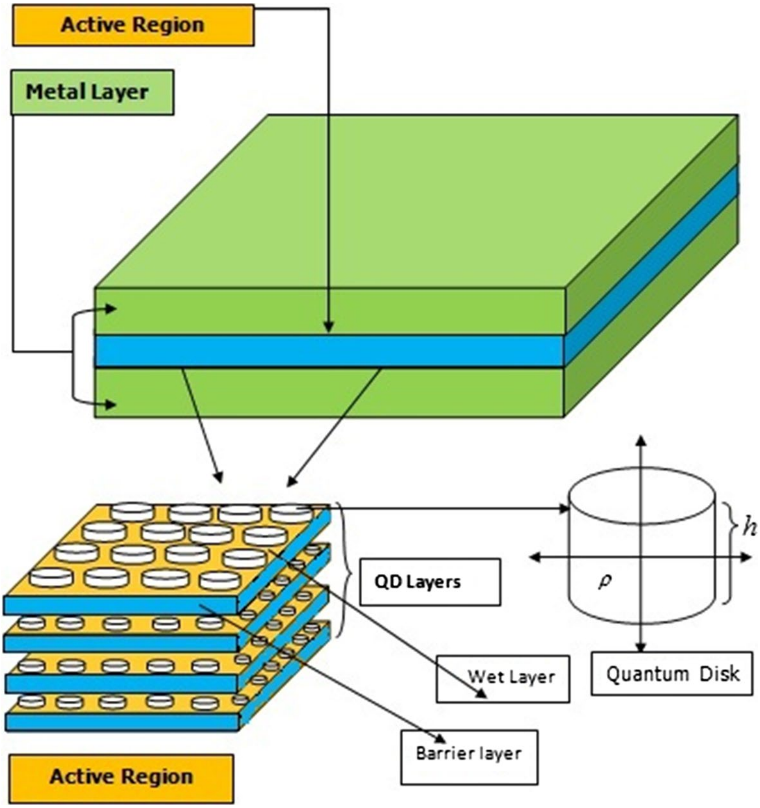

Fig. 1 Active region of plasmonic QD nanolaser structure

6 Results and discussions

The data used in the calculations were stated in Table 1. Figure 2 shows the real (red curve) and complex (blue curve) parts of the dielectric function $\varepsilon_m(\omega)$ for silver (Ag-metal). The real part has a high negative value due to free-electron contribution, while imaginary part has small positive value and becomes zero 1.45 eV. This is exactly the behavior of the dielectric function at infrared (Baltar et al. 2012). These results coincide with Das et al. (2016) for the silver dispersive curve.

The dielectric function of semiconductors is different from that of metal. Figure 3 displays real and imaginary parts of the dielectric function of QDs $\varepsilon_{QD}(\omega)$. At low photon energies near 0.8 eV, the real part of $\varepsilon_{QD}(\omega)$ has high value and decrease at high energies. The imaginary part of $\varepsilon_{QD}(\omega)$ (blue curve) has a low value compared with the real part and also decreases at high energies. This is with the assumption that $\varepsilon''_{QD} = 0$ referred to above in Sect. 2. Figure 4 shows the dielectric function of the plasmonic QD structure under study. Its real part has a high positive value which comes from the QD contribution shown in Fig. 3. The curve shape is different from that of QD and its value is less as a result of metal contribution.

Figure 5 display propagation constant of SPPs (k_{spp}) at the interface of Ag metal/InAs QD structure. The value of the imaginary part (blue curve) of k_{spp} is in the range of that of

Table 1 Some of the parameters used to simulate plasmonic QD nanolaser. Some of the calculated states are also listed

Parameter	Value	Unit
Bandgap energy of InAs QD	0.354	eV
Background refractive index of InAs QD	$n_b = 1.5$	
Electron effective mass	$0.023m_0$	
Heavy hole mass of InAs	$0.4m_0$	
Electron effective mass of InGaAs	$0.03m_0$	
Heavy hole mass of InGaAs	$0.46m_0$	
Electron effective mass of GaAs	$0.067m_0$	
Heavy hole effective mass of GaAs	$0.333m_0$	
Electron effective mass of Ag metal	$0.99m_0$	
Heavy hole effective mass of Ag metal	m_0	
Barrier layer thickness	$t_B = 10$	nm
Ag metal layer thickness	$t_M = 3$	nm
Ag work function	$Q_m = 4.64$	eV
Ariel density of QDs	$N_d = 5 \times 10^{12}$	m^{-2}
disc height	$h = 3$	nm
Carrier density	$n_{2d} = 3 \times 10^{12}$	m^{-2}
Spectral variance of QDs	$\sigma = 0.05$	eV
Variance of the linewidth	$\gamma = 0.05$	eV
Calculated parameters through this work		
CB edge of barrier	1.0906	eV
VB edge of barrier	– 0.3335	eV
CB edge of Ag metal	2.7298	eV
VB edge of Ag metal	– 1.2433	eV
CB edge of InGaAs WL	1.0631	eV
VB edge of InGaAs WL	– 0.1869	eV

the dielectric medium, while the real part value (red line) of k_{spp} is in the range of metal. Above plasma frequency w_p, the absolute value of Re(k_{spp}) is larger than Im (k_{spp}). This is an acceptable result since the neglected absorption (i.e. dispersion or real part becomes important) corresponds to metal while high absorption is adequate for dielectric contribution which is contrary to the real part (dispersion). Results in Fig. 5 are in agreement with Baltar et al. (2012).

Figure 6 illustrates the dispersion relation of the plasmonic QD structure at a frequency far below the plasma one (w_p). It was shown that at frequencies smaller than w_p the gap between real and imaginary parts was large and a deviation from linear relation was obvious. Both curves simulate the absorption (gain) and dispersion curves of the QDs. This may be due to its high contribution in this frequency regime. Near $1/2w_p$, the gap decreases and the curves begin coincides which refer to the region of the dominance of metal characteristics.

Figure 7 express, respectively, the dispersion relations of the real (Fig. 7a) and imaginary (Fig. 7b) parts of the SPP propagation constant k_{spp} at the Ag/InAs-QD (red curve) and Ag/Air (blue curve) interfaces. In these figures, the value of the dielectric constant of air is taken as ($\varepsilon = 1$). One of the most important features of SPPs is the behavior near the surface-plasmon frequency, and here appears at $\omega/\omega_p \sim 0.37$. At this value, the

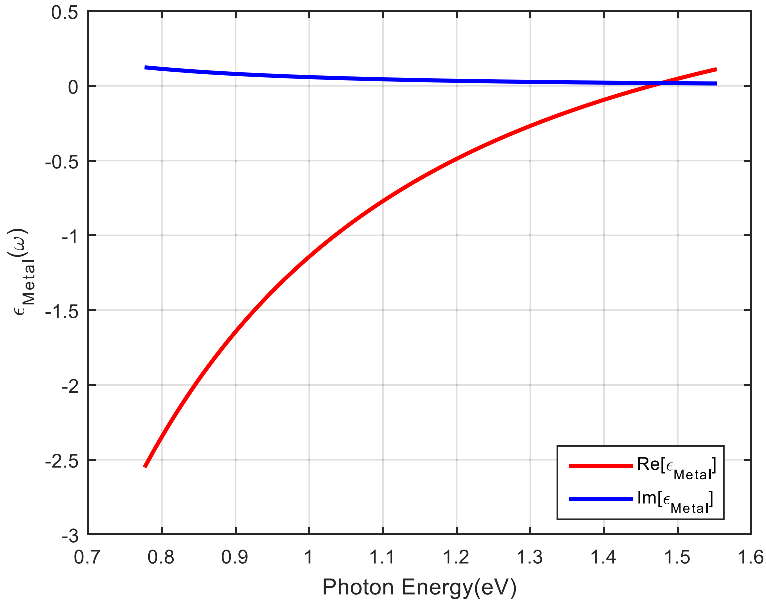

Fig. 2 Dielectric function of Ag metal. (Color figure online)

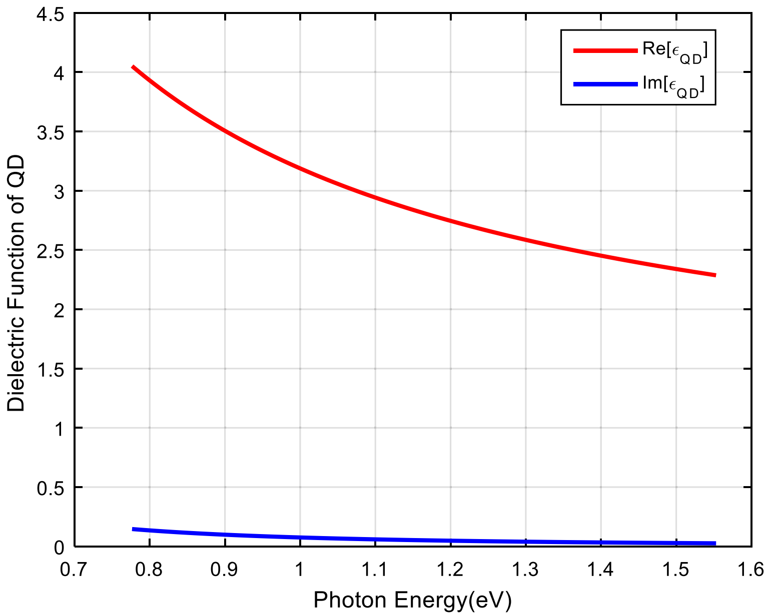

Fig. 3 Dielectric function of InAs-QD. (Color figure online)

propagation constant along the interface increased enormously than that of the Ag/Air by more than three orders in the two figures. This is acceptable since the real part of the dielectric function ε_{QD} was larger than that of metal ε_m (as in Figs. 2 and 3), which in

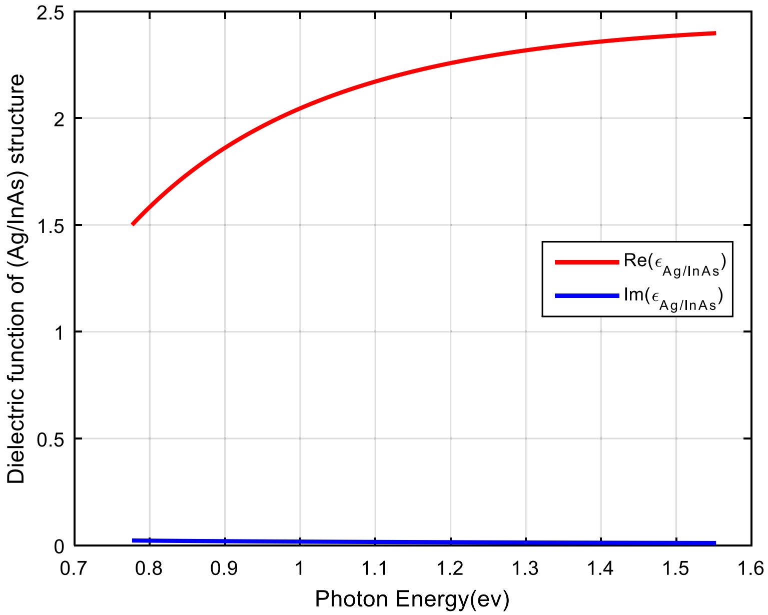

Fig. 4 Dielectric function of metal-Ag/InAs-QD structure. (Color figure online)

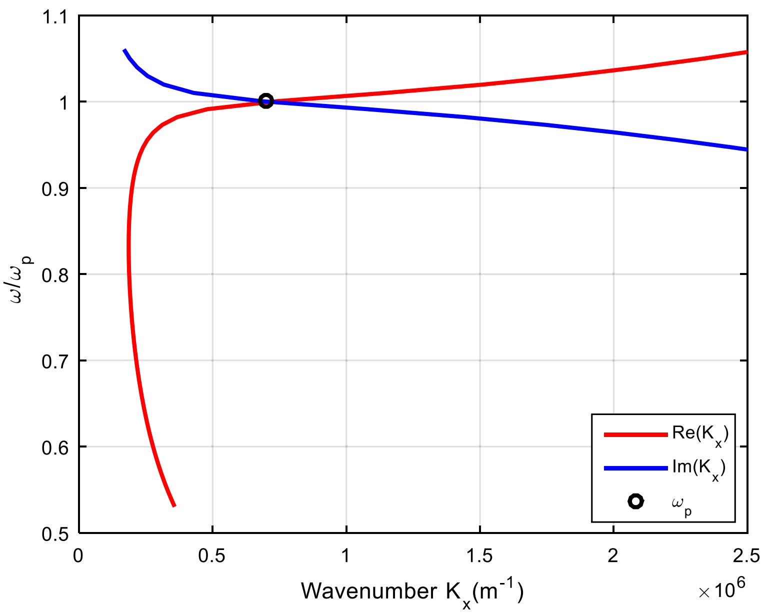

Fig. 5 Propagation constant of SPPs in metal-Ag/InAs-QD structure. (Color figure online)

turn leads to increase the optical transmittance of metal (Ag) or lowest its absorption (Al-Husseini and Al-Khursan 2009). This result is in agreement with Berini and Leon (2012) for Ag/dielectric, and Vargas (2017) for Ag/air. Figure 7 also shows that the peak of k_{spp}

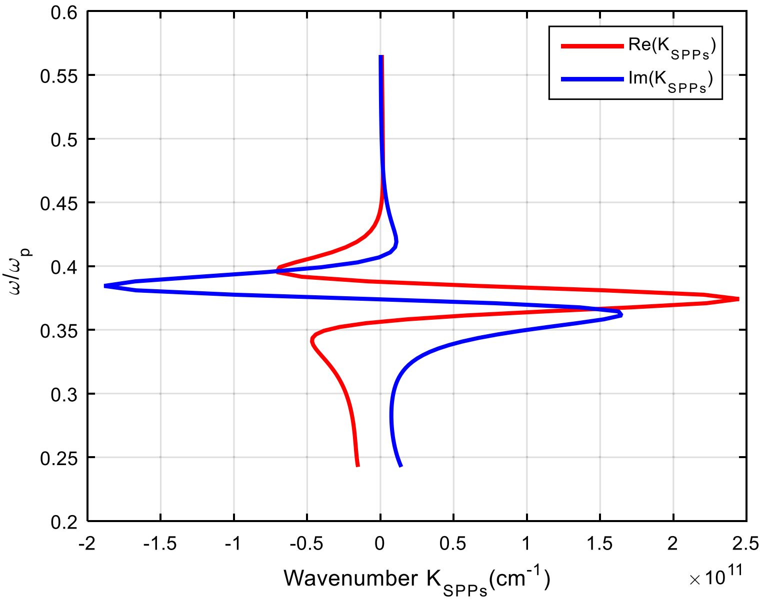

Fig. 6 Propagation constant of SPPs in metal-Ag/InAs-QD structure at far below the plasma frequency. (Color figure online)

corresponds to a very short wavelength, i.e. SPPs wavelength is very short compared with the peak emitted wavelength of photons.

Figure 8 displays the skin depth spectrum for SPP waves, δ_{spp}, at the interface of the metal-Ag/InAs-QD structure. It shows how the electric field decays exponentially. A knee is shown at the plasma resonance w_p of Ag. The skin depth is gradually decreased towards the metal surface. Form the inset of Fig. 8 one can refer that near plasma frequency of Ag metal, δ_{spp} not accedes 50 nm i.e. the SPP field was strongly localized at the interface. Localized SPPs in the zero-dimensional structures have applications in the surface-enhanced Raman scattering in the super-resolution and best sensitivity in optical imaging (Okamoto 2011).

Figure 9 indicates the propagation length of SPP, L_{spp}, into Ag/InAs-QD interface (blue curve). The curve of the Ag/Air interface (red dotted curve) was also shown, for comparison. It is shown that L_{spp} at the Ag/InAs-QD interface was much larger than that in the Ag/Air interface. This means that SPP mode was well confined in the Ag/InAs-QD interface while the damping in the SPP energy was high in the Ag/Air interface. The range of L_{spp} values was in the range of that in the literature, for example, He et al. (2012).

7 Conclusions

The dielectric function in the plasmonic QD nanolaser was modeled and studied for an MSM structure. This was to attain plasmonic nanocavity covered by Ag metal with active region contains: QD, wetting layer (WL) and barrier. Parameters like: propagation length, skin depth and propagation constant for SPP were studied. The dispersion relation of the plasmonic QD structure was evaluated. The gap between real and imaginary parts was large

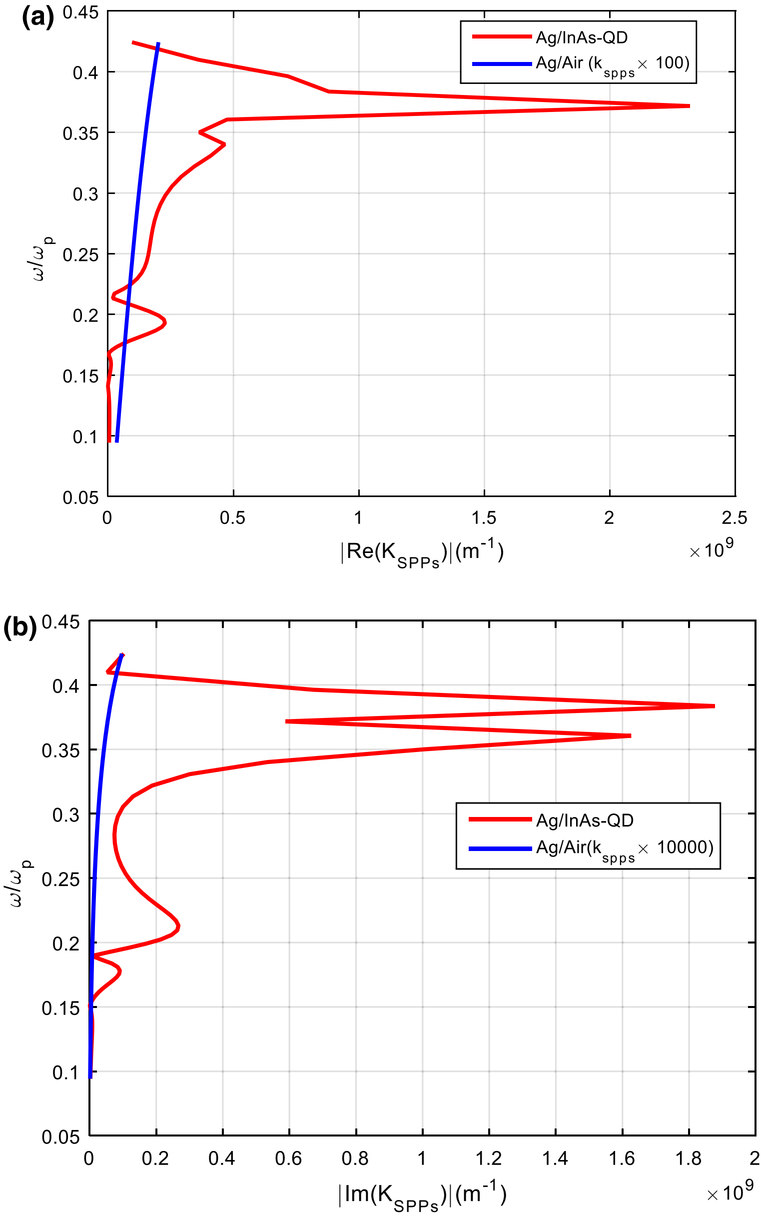

Fig. 7 **a** Real and **b** imaginary parts of k_{spp} at metal-Ag/InAs-QD (red curve) and Ag/Air (blue curve) interfaces, respectively. (Color figure online)

and a deviation from linear relation was obvious at frequencies smaller than w_p. At the half of w_p the gap was decreased due to metal contribution dominance. At $\omega/\omega_p \sim 0.37$, then k_{spp} for Ag/InAs-QD was increased enormously than the Ag/air interface by more than three orders. The skin depth, δ_{spp}, does not exceed 50 nm i.e. the SPP field was strongly localized at the interface due to the effect of zero-dimensional QD structure which has

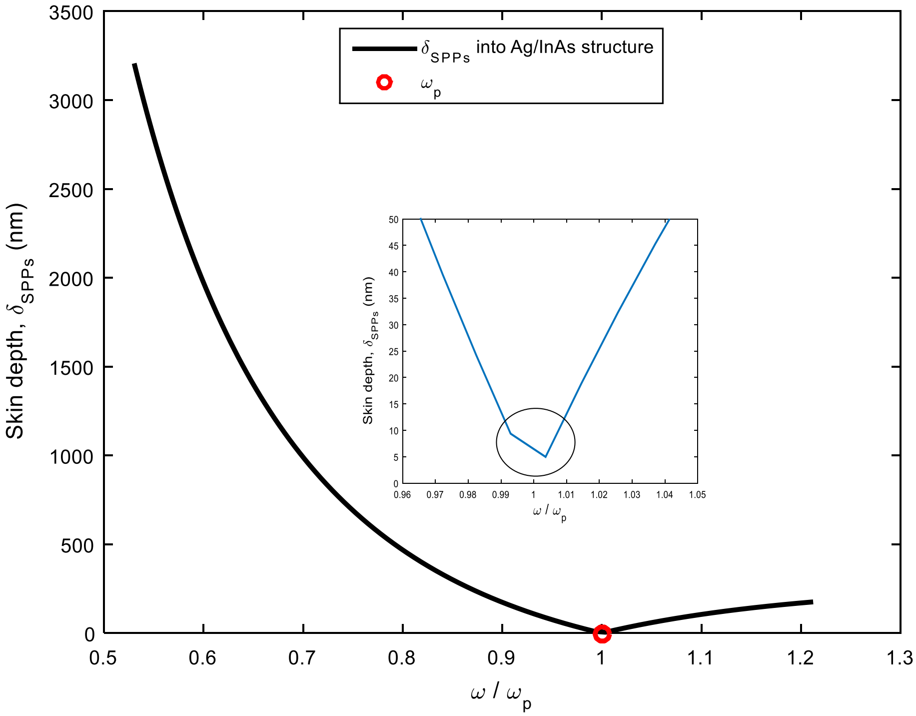

Fig. 8 Skin depth of SPPs at metal-Ag/InAs-QD interface

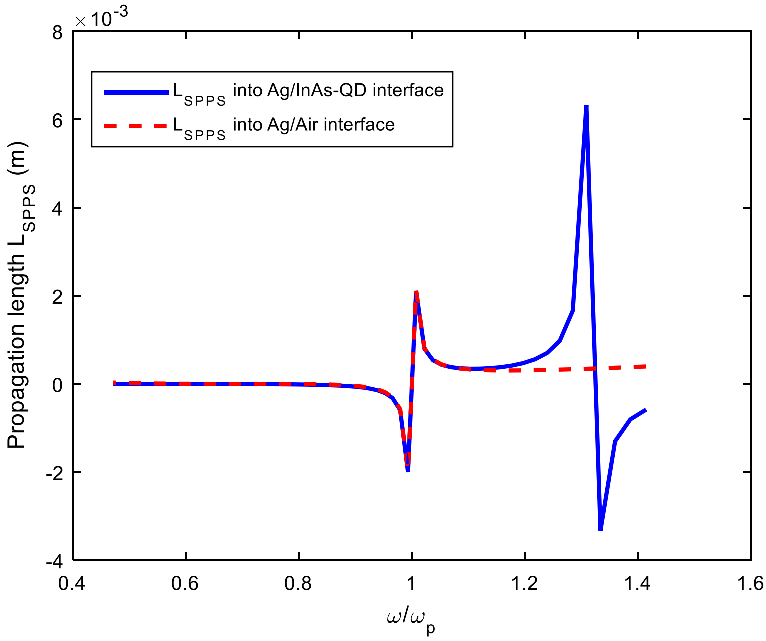

Fig. 9 The propagation length L_{spp} at metal-Ag/InAs-QD (blue curve) and Ag/Air (red dotted curve) interfaces. (Color figure online)

application in the super-resolution and best sensitivity in optical imaging. The results of the propagation length of SPP, L_{spp}, also support this. L_{spp} results also refer that the damping in the Ag/QD interface was low compared to that in the Ag/air interface. The obtained results are in the range of experimental ones.

References

Abdullah, M., Noori, F.T.M., Al-Khursan, Amin H.: Terahertz emission in ladder plus Y-configurations in double quantum dot structure. Appl. Opt. **54**, 5168–5192 (2015)

Al-Khursan, A.H.: Gain of excited states in the quantum-dots. Physica E **35**, 6–8 (2006)

Al-Husseini, H., Al-Khursan, A.H., Al-Dabagh, S. Y.: III-Nitride QD Lasers. The Open Nanosci J **3**(1), 1–11 (2009)

Baltar, H., Drozdowicz-Tomsia, K., Goldys, E.: Propagating surface plasmons and dispersion relations for nanoscale multilayer metallic-dielectric films. In: Kim, K.Y. (ed.) Plasmonics-Principles and Applications. IntechOpen, Rijeka (2012). https://doi.org/10.5772/51218

Berini, P., Leon, I.D.: Surface plasmon–polariton amplifiers and lasers. Nat. Photon. **6**, 16–24 (2012)

Bimberg, D., Kirstaedter, N., Ledentsov, N.N., Alferov, ZhI, Kopev, P.S., Ustin, V.M.: In GaAs–GaAs quantum-dot lasers. IEEE J. Sel. Top. Quantum Electron. **3**, 196–205 (1997)

Chen, L.F., Ong, C.K., Neo, C.P., Varadan, V.V., Varadan, V.K.: Microwave Electronics Measurement and Materials Characterization. Wiley, Hoboken (2004)

Das, G., Coluccio, M.L., Alrasheed, S., Giugni, A., Allione, M., Torre, B., Perozziello, G., Candeloro, P., Fabrizio, E.Di: Plasmonic nanostructures for the ultrasensitive detection of biomolecules. Rivista Del Nuovo Cimento **39**, 547–586 (2016)

Dionne, J.A., Sweatlock, L.A., Atwater, H.A.: Planar metal plasmon waveguides: frequency-dependent dispersion, propagation, localization, and loss beyond the free electron model. Phys. Rev. B **72**, 075405 (2005)

Dwara, S.N., Al-Khursan, A.H.: Quantum efficiency of InSbBi quantum dot photodetector. Appl. Opt. **54**, 9722–9727 (2015)

Han, Y.J., Li, L.H., Zhu, J., Valavanis, A., Freeman, J.R., Chen, L., Rosamond, M., Dean, P., Davies, A.G., Linfield, E.H.: Silver-based surface plasmon waveguide for terahertz quantum cascade lasers. Opt. Express **26**, 3814–3827 (2018)

He, X.Y., Wang, Q.J., Yu, S.F.: Numerical study of gain-assisted terahertz hybrid plasmonic waveguide. Plasmonics **7**, 571–577 (2012)

Holmström, P., Thylén, L., Bratkovsky, A.: Dielectric function of quantum dots in the strong confinement regime. J. Appl. Phys. **107**, 064307 (2010)

Homola, J.: Present and future of surface plasmon resonance biosensors. Anal. Bioanal. Chem. **377**, 528–539 (2003)

Homola, J.: Surface Plasmon Resonance Based Sensors. Springer, Berlin (2006)

Kim, J., Chuang, S.L.: Theoretical and experimental study of optical gain, refractive index change, and linewidth enhancement factor of p-doped quantum-dot lasers. IEEE J. Quantum Electron. **42**, 942–952 (2006)

Kim, J., Laemmlin, M., Meuer, C., Bimberg, D., Eisenstein, G.: Static gain saturation model of quantum-dot semiconductor optical amplifiers. IEEE J. Quantum Electron. **44**, 658–666 (2008)

Kittel, C.: Introduction to Solid State Physics, 8th edn. Wiley, Hoboken (2005)

Li, D.B., Ning, C.Z.: Giant modal gain, amplified surface plasmon-polariton propagation, and slowing down of energy velocity in a metal-semiconductor-metal structure. Phys. Rev. B **80**, 153304 (2009)

Lüth, H.: Solid Surfaces, Interfaces and Thin Films. Springer, Berlin (2015)

Maier, S.A.: Plasmonics: Fundamentals and Applications. Springer, New York (2007)

Mishchenko, M.I., Travis, L.D., Lacis, A.A.: Scattering, Absorption and Emission of Light by Small Particles. Cambridge University Press, Cambridge (2002)

Ni, C.A., Chang, S., Gargas, D.J., Moore, M.C., Yang, P., Chuang, S.L.: Metal-coated zinc oxide nanocavities. IEEE J. Quantum Electron. **47**, 245–251 (2011)

Okamoto, K.: Surface plasmon enhanced solid-state light-emitting devices. In: Wang, Z.M., Neogi, A. (eds.) Lecture Notes in Nanoscale Science and Technology, Nanoscale Photonics and Optoelectronics, pp. 27–46. Springer, Berlin (2011). https://doi.org/10.1007/978-1-4419-7587-4_2

Raether, H.: Surface Plasmons on Smooth and Rough Surfaces and on Gratings. Springer, Berlin (1988)

Rakic, A.D., Djurisic, A.B., Elazar, J.M., Majewski, M.L.: Optical properties of metallic films for vertical-cavity optoelectronic devices. Appl. Opt. **37**, 5271–5283 (1998)
Sernelius, B.E.: Surface modes in physics. Wiley, Hoboken (2001)
Vargas, W.E.: Dielectric functions of Pd and Zr transition metals: an application of Drude-Lorentz models with simulated annealing optimization. Appl. Opt. **56**, 1266–1275 (2017)
Wijesinghe, T., Premaratne, M.: Dispersion relation for surface plasmon polaritons on a Schottky junction. Opt. Express **20**, 7151–7164 (2012)
Wu, B., Mathews, N., Sum, T.-C.: Plasmonic Organic Solar Cells: Charge Generation and Recombination. Springer, Singapore (2017)
Zeng, S., Baillargeat, D., Ho, H.-P., Yong, K.-T.: Nanomaterials enhanced surface plasmon resonance for biological and chemical sensing applications. Chem. Soc. Rev. **43**, 3426–3452 (2014)